JOURNAL OF MATERIALS SCIENCE **40** (2005) 719–723

Static and dynamic magnetic properties of Co_2Z barium ferrite nanoparticle composites

Z. W. LI, L. CHEN
Temasek Laboratories, National University of Singapore, 10 Kent Ridge Crescent, Singapore, 119260
E-mail: tsllizw@nus.edu.sg

C. K. ONG
Center for Superconducting and Magnetic Materials and Department of Physics, National University of Singapore, 10 Kent Ridge Crescent, Singapore, 119260

Z. YANG
Research Institute of Magnetic Materials, Lanzhou University, Lanzhou, People's Republic of China, 730000

The static, dynamic and attenuation properties of Co_2Z barium ferrites and Co_2Z composites have been studied. The results showed that both static and dynamic magnetic properties are significantly different for large particles and nanoparticles. As compared to large particles, Co_2Z nanoparticles have a small saturation magnetization M_s, large coercivity H_c, small permeability μ'_0 and μ''_{max}, but high resonance frequency f_R . The maximum reflection loss predicted is much smaller for nanoparticles than for large particles. Therefore, Co_2Z barium ferrite with large particle is more suitable for EM materials with high attenuation and broad bandwidth at microwave frequency.

1. Introduction

Over the past decade, magnetic nanoparticles have attracted much attention due to their very valuable properties from both application and theory point of view. The nanoparticles have many special magnetic and electrical properties that are significantly different from large particles. The saturation magnetization of nanoparticles is found to be smaller than the bulk values for spinel [1, 2] and barium ferrites [3, 4]. The Néel temperature was elevated as compared to bulk materials [5]. Morrish *et al.* [6] have demonstrated that the elevated Néel temperature was attributed to an increased iron occupancy on the A site in spinel ferrite. This in turn leads to an increase in the total superexchange interaction. Also, the magnetic nanoparticles have numerous potential and practical applications, such as perpendicular recording media [7, 8] and two-phase permanent alloys [9, 10].

For magnetic nanoparticles, most studies concentrated on the static properties, but only a few on the dynamic properties. As we know, electromagnetic (EM) composites have been used extensively in defense, industry and commerce. Due to the strong absorption of EM wave, the materials can be used in high-speed electronic circuits or other devices to minimize environmental EM interference, decrease the noise level in signals, and ensure EM compatibility. Such composite materials are usually comprised of a ferrite and a polymer. The studies on the dynamic magnetic properties, such as complex permeability and resonance frequency, are of great interest [11–13]. In this paper, we will report on the static and dynamic magnetic properties of Co_2Z barium ferrite ($Ba_3Co_2Fe_{24}O_{41}$) and its composites, as well as the attenuation properties at microwave frequencies for large particles and nanoparticles.

2. Experimental

Co_2Z barium ferrite nanoparticles were synthesized using chemical co-precipitation. The Co_2Z nanoparticles were ball-milled at various durations, followed by annealing at 600°C for 2 h to remove the stress and eliminate the crystal imperfection due to ball-milling. In addition, the nanoparticles were shaped and sintered at 1300°C to obtain large grain sizes of a few micrometer (known as large particles). The number of samples and the corresponding preparation methods are listed in Table I.

The composite samples were prepared by mixing the fine powders of Co_2Z with epoxy resin. The volume concentration of the powders is 35% for all composites. Next, they were fabricated into cylinders with an outer diameter of 6.9 mm, inner diameter of 3 mm and length of about 2 mm for the microwave measurements.

The X-ray diffraction measurements were performed using a Philips diffractometer with Cu K_α radiation. The magnetization curves and *M-H* loops were measured with applied fields of 0–80 kOe, and between −20 and

TABLE I Preparation, grain size, saturation magnetization M_s, coercivity H_c and high field susceptibility χ_p for Co_2Z barium ferrite

No.	Preparation	Size (nm)	M_s (emu/g)	H_c (Oe)	χ_p (emu/g/kOe)
#0	Original	75	49.4	180	0.0325
#1	Ball-mill 1.5 h	38	47.7	392	0.0402
#2	Ball-mill 4 h	30	45.2	420	0.0409
#3	Ball-mill 8 h	20	40.2	450	0.0488
#4	Anneal at 1300°C	10 μm	55.3	45	0.0215

+20 kOe, respectively, at room temperature using VSM from Oxford Instruments. The real and imaginary parts of the permeability over 0.5 to 16.5 GHz were measured using the transmission/reflection method based on algorithms developed by Nicolson and Ross [14], and by Weir [15]. The measurement fixture is a set of 7 mm coaxial air-line with length of 59.96 mm. The microwave measurement was conducted using a HP8722D Vector Network Analyzer.

3. Results and discussion

3.1. Structural characteristics

Some typical X-ray diffraction patterns with the scanning 2θ angles from 20° to 80° are shown in Fig. 1a. The X-ray diffraction showed that all samples are single phase with Z-type hexagonal-ferrite structure. However, a small amount of other phases was also detected. As compared to sample #4, the diffraction lines are obviously broad for the original co-precipitation powders and the ball-milled powders. The patterns with scanning 2θ angles from 61° to 64.5° are shown in Fig. 1b for samples with ball-milling time of 1.5, 4 and 8 h. With increasing ball-milling time, the (220) line of the samples becomes broader. The apparent grain sizes can be estimated from the width of the (220) lines based on the Scherrer formula. Next, the average hexagonal diameters of the grains were obtained using the method proposed by Pernet *et al.* [16]. It is obvious that as the ball-milling time increases, the grain sizes decreases from 75 to 20 nm, as shown in Table I. In addition, the grain size of sample #4 was about 10 μm, obtained from SEM image.

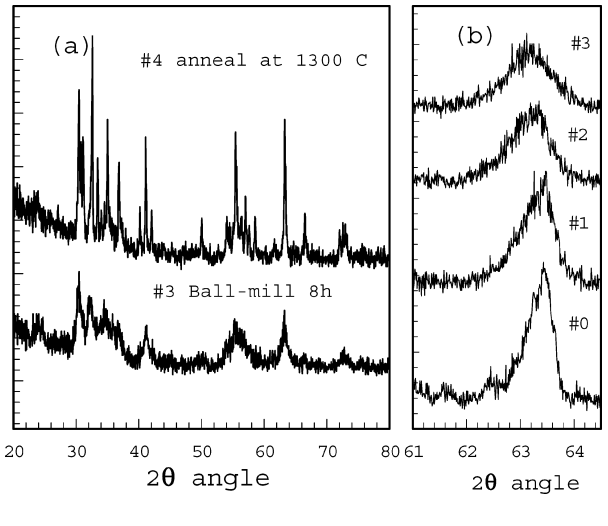

Figure 1 Some typical x-ray diffraction patterns for Co_2Z barium ferrites; the scanning 2θ are (a) from 20 to 80° and (b) from 61 to 64.5°

3.2. Magnetic properties

Magnetization curves are shown in Fig. 2 for Co_2Z ferrites with various grain sizes. The saturation magnetizations M_s were deduced from numerical analysis of the magnetization curves based on the law of approach to saturation [17]. The coercivities H_c were obtained from the *M-H* loops. The values of M_s and H_c are listed in Table I for various sizes d. The saturation magnetization and coercivity are 55.3 emu/g and 45 Oe for large particles, respectively. The values of M_s is slightly larger than 50 emu/g, as reported by Sugimoto *et al.* [18]. For nanoparticles, as the grain sizes decrease from 75 nm to 20 nm, the saturation magnetizations decrease from 49.4 emu/g to 40.2 emu/g, while the coercivities increase from 180 Oe to 450 Oe.

The decrease in M_s for the nanoparticles can be interpreted by considering the core-surface model [19]. In the model, the crystal grain can be divided into two parts, namely, the core and the surface layer, with significantly different magnetic properties. For a spherical grain of diameter d and surface thickness t, let M_{s1} and M_{s2} be the saturation magnetizations of the core and surface, respectively, with the corresponding volumes v_1 and v_2. The total saturation magnetization M_s is given by

$$M_s = \frac{M_{s1}v_1 + M_{s2}v_2}{v_1 + v_2} = M_{s1} - \frac{6t}{d}(M_{s1} - M_{s2}) \quad (1)$$

The saturation magnetizations M_s, plotted as a function of the reciprocal of grain size $1/d$, are shown in Fig. 3a. It is found that a good linear relationship exists between M_s and $1/d$. From the straight line, we obtain $M_{s1} = 55.1$ emu/g at $1/d = 0$, which is consistent with 55.3 emu/g for large particles. On the other hand, from the slope of the line, we obtain $M_{s2} = M_{s1} - \alpha/6t$, where $\alpha = 330.4$ nm · emu/g. This implies that the magnetization is significantly smaller for the surface layer than for the core. If it is assumed that the thickness of the surface layer is 2–3 nm, the saturation magnetization of the surface layer is calculated to be between 27.6 and 36.7 emu/g. The large decrease in the saturation magnetization of the surface layer has several potential sources, including crystal imperfection on the surface layer, reduction in superexchange interactions [20, 21] and non-collinear magnetic structure [22–25]. The high field susceptibility χ_p is only 0.0215 emu/g/kOe for large particles, but rapidly increases for nanoparticles, as shown in the inset of Fig. 2. This implies that a non-collinear magnetic structure (spin canting) occurs and the average canting angle increases with decreasing grain sizes.

The coercivity H_c is very sensitive to the grain size. The inverse relationship between H_c and grain size d has been extensively reported for NiZn, MnZn and Co spinel ferrites [26, 27], YIG garnet [28] and barium

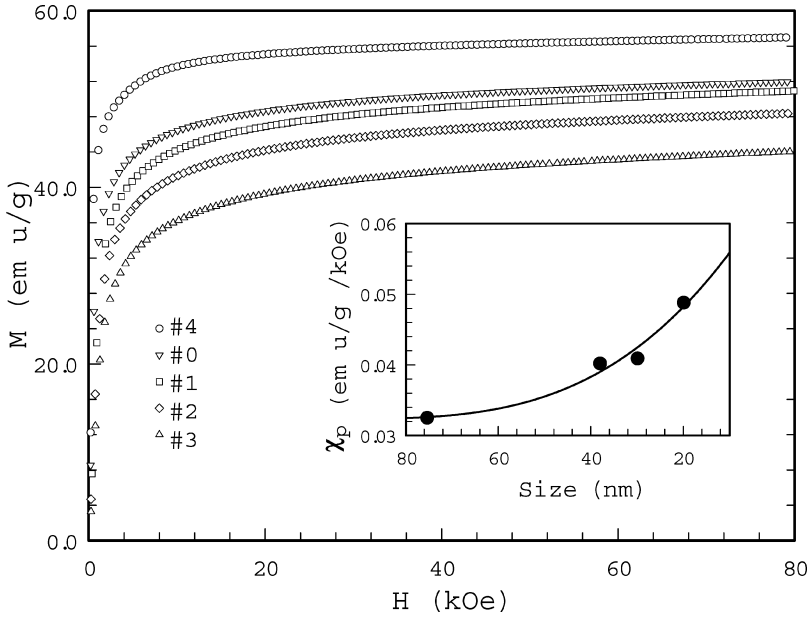

Figure 2 Magnetization curves for Co_2Z barium ferrite with various grain sizes; the inset shows the high field susceptibility χ_p.

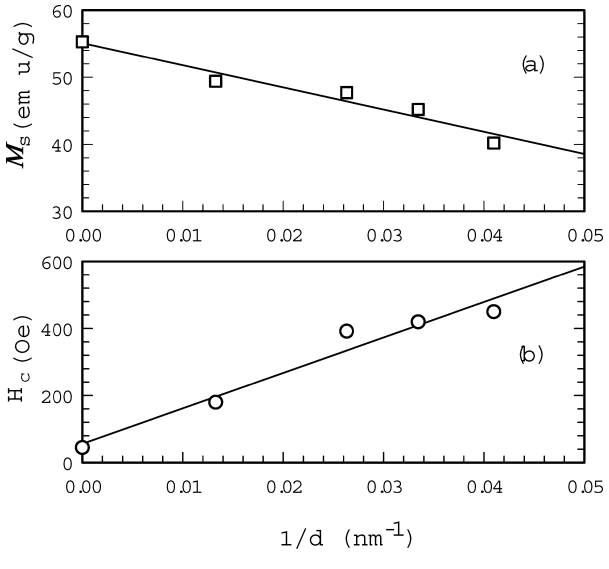

Figure 3 The open squares and circles are the dependence of (a) saturation magnetizations M_s and (b) coercivities H_c on the reciprocal of grain sizes d, respectively.

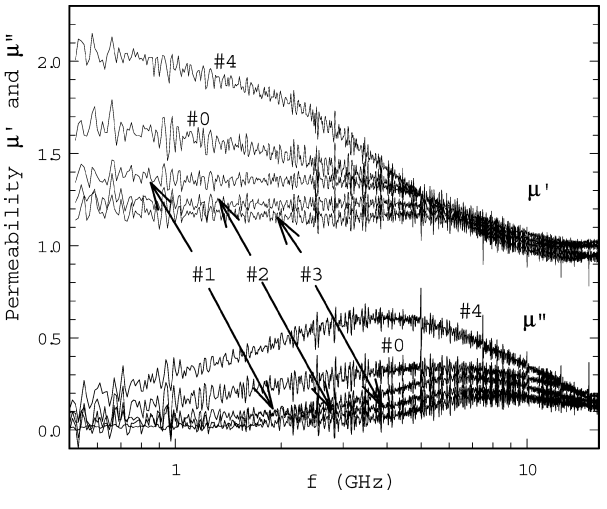

Figure 4 Permeability spectra from 0.5 to 16.5 GHz for Co_2Z composites with various grain sizes.

ferrites [29]. The same relationship is also observed for Co_2Z nanoparticles, as shown in Fig. 3b. The other causes may be stress and surface anisotropy. The ball-milled samples retain a large stress, which cannot be removed completely by annealing. The stress can lead to large coercivity. In addition, Morrish *et al.* have indicated that anisotropy is larger in the surface layer of particles than in the core [19]. Therefore, as the grain size decreases, the ratio of the surface layer to the total volume increases, leading to increase in the coercivity for nanoparticles.

3.3. Dynamic magnetic properties

The permeability spectra from 0.5 to 16.5 GHz are shown in Fig. 4 for Co_2Z composites with 35% volume concentration. The permeability μ_0' (defined as the real value at 0.5 GHz), the maximum of the imaginary value μ''_{max} and the resonance frequency f_R are listed in Table II. The real and imaginary values of permittitivity, ϵ' and ϵ'', are almost constant over the measured frequency range. The values are also listed in Table II.

The values of μ_0' and μ''_{max} are 2.05 and 0.60, respectively, for large particles, which are larger than the corresponding values for nanoparticles. However, the resonance frequency f_R of 3.5 GHz is smaller than

TABLE II Dynamic properties for Co_2Z composite with 35% volume concentration of ferrite particles

No.	f_R (GHz)	μ_0'	μ''_{max}	ϵ'	ϵ''
#4	3.5	2.05	0.60	6.8	0.9
#0	4.5	1.65	0.35	6.9	1.0
#1	6.5	1.40	0.30	5.3	0.2
#2	7.5	1.25	0.20	5.3	0.2
#3	8.0	1.20	0.20	5.4	0.3

that of nanoparticles. In addition, as the grain size of nanoparticles decreases from 0.75 nm to 0.20 nm, μ_0' and μ''_{max} decrease from 1.65 to 1.20 and from 0.35 to 0.20, respectively, while the resonance frequency f_R increases from 4.5 to 8.0 GHz.

The decrease in permeability μ_0' is due to several possible factors. First, it is known that the permeability is proportional to the saturation magnetization M_s and inversely proportional to the coercivity H_c. Small M_s and larger H_c lead to a small permeability μ_0' for nanoparticles, as compared to large particles. A more important factor is the demagnetizing field in the composites. In the case of spherical barium ferrite particles embedded in an infinite and homogeneous epoxy matrix, magnetic poles are created on the surface of ferrite particles in an applied magnetic field, thus producing the demagnetizing field, whose direction is opposite to that of the applied field. The magnitude of the demagnetizing field is relative to the amount of surface magnetic charges. For a given volume concentration, as the particle sizes of barium ferrite decrease, surface charges will increase. This gives rise to a larger demagnetizing field in the composites. Hence, the permeability μ_0' decreases due to a large demagnetizating field for composites with small size particles. A crude estimation on the demagnetizing effect can be made based on the magnetic circuit model [30]

$$\frac{1}{\mu'_{0,\text{bulk}} - 1} = \frac{1}{\mu_0' - 1} - N \tag{2}$$

where N is the effective demagnetizing factor of the composite, and $\mu'_{0,\text{bulk}}$ is the permeability of bulk material or particles. It is obvious from Equation 2 that the permeability of the composite μ_0' is associated with the effective demagnetizing factor N. Therefore, the composites with nanoparticle have a small μ_0' due to the large N.

On the other hand, the resonance frequency f_R can be written as

$$f_R = \frac{\gamma}{2\pi} H_{\text{eff}} \tag{3}$$

where $\gamma/2\pi = 2.8$ MHz/Oe is the gyromagnetic ratio, and H_{eff} is the effective magnetic field, which includes the anisotropy field H_a and the demagnetizing field H_d. Particles of small size have a large demagnetizing field, which leads to a high resonance frequency based on Equation 3. Therefore, the demagnetizing field plays a dominant role in decreasing the permeability μ_0' and increasing the resonance frequency f_R for nanoparticles.

3.4. Attenuation properties

EM wave attenuation is determined from the reflection loss (RL). In the case of a metal-backed single layer, RL is given by

$$\begin{cases} RL(dB) = 20 \log_{10} |(Z_{\text{in}} - Z_0)/(Z_{\text{in}} + Z_0)| \\ Z_{\text{in}} = Z_0 \sqrt{\mu/\epsilon} \tanh[j(2\pi f t/c)\sqrt{\mu\epsilon}] \end{cases} \tag{4}$$

where Z_{in} is the impedance of composites, $Z_0 = 1$ is the normalized impedance of free space, c is the light velocity, $t = 0.4$ cm is the thickness of the composite, f is the frequency of the incident EM wave, $\mu = \mu' - j\mu''$ is the complex permeability and $\epsilon = \epsilon' - j\epsilon''$ is the complex permittivity. The real and imaginary values of permittivity are taken from Table II. The values of permeability are obtained from Fig. 4. The calculated reflection loss are shown in Fig. 5 for Co_2Z composites with various grain sizes. As compared to a reflection loss of -32 dB for large particle (#4), the maximum reflection loss of nanoparticles are only -18, 9.5, 6 and 5.5 dB for sample #0, #1, #2 and #3, respectively. The band width for 10 dB attenuation reduces from 3.6 GHz for large particles (#4) to 2.2 GHz for nanoparticles (#0).

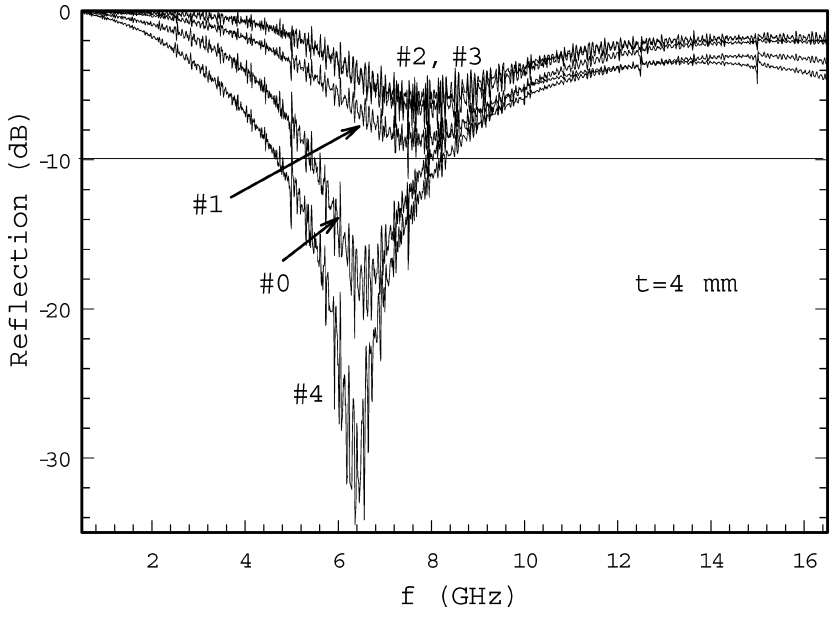

Figure 5 Reflection loss over 0.5 to 16.5 GHz for Co_2Z composites with various grain sizes.

It is known that broadband reflection loss is determined by two conditions. In order to have EM wave incident on a composite, it is necessary to achieve impedance match between the composite and free space, which is mainly dependent on the ratio of $\sqrt{\mu/\epsilon}$. When the EM wave is inside the composite, the absorption of EM energy is determined by the magnitude of $\mu''_{\max}$. Therefore, for nanoparticles, small μ'_0 and $\mu''_{\max}$ lead to low reflection loss over narrow band, as compared to that of large particles.

4. Conclusions

Co_2Z nanoparticles have a small saturation magnetization M_s, large coercivity H_c, small permeabilities μ'_0 and $\mu''_{\max}$, but high resonance frequency f_R, as compared to that of large particles. The maximum reflection loss is much smaller for nanoparticles than for large particles. Therefore, as compared to nanoparticles, Co_2Z barium ferrite with large particles is more suitable for EM materials with low reflectivity over wide bandwidth at microwave frequency.

References

1. A. H. MORRISH and K. HANEDA, *J. Appl. Phys.* **52** (1981) 2496.
2. K. HANEDA and A. H. MORRISH, *ibid.* **63** (1988) 4258.
3. H. YAMADA, M. TAKANO, M. KIYAMA, J. TAKADO, T. SHINJO and K. WATANABE, *Adv. Ceramics* **16** (1986) 169.
4. S. KURISU, T. ITO and H. YOKOYAMA, *IEEE Trans. Magn.* **23** (1987) 313.
5. Z. X. TANG, C. M. SORENSEN, K. J. KLABUNDE and G. C. HADJIPANAYIS, *Phys. Rev. Lett.* **67** (1991) 3602.
6. A. H. MORRISH, Z. W. LI and X. Z. ZHOU, *J. Phys. IV France* **7** (1997) C1-513.
7. O. KUBO, T. IDO and H. YAKOYAMA, *IEEE Trans. Magn.* **18** (1982) 1122.
8. Z. YANG, J. H. ZHAO, H. X. ZENG and G. YAN, *Int. J. Soc. Mater. Eng. Resour.* **3** (1995) 203.
9. J. DING, P. G. MCCORMICK and R. STREET, *J. Magn. Magn. Mater.* **124** (1993) 1.
10. Z. W. LI, X. Z. ZHOU, A. H. MORRISH and B. G. SHEN, *Hyperfine Interac.* **72** (1992) 111.
11. T. NAKAMURA, T. TSUTAOKO and K. HATAKEYAMA, *J. Magn. Magn. Mater.* **138** (1994) 319.
12. D. Y. KIM, Y. C. CHUNG, T. W. KANG and H. C. KIM, *IEEE Trans. Magn.* **32** (1996) 555.
13. HAN-SHIN CHO and SUNG-SOO KIM, *ibid.* **35** (1999) 3151.
14. A. M. NICOLSON and G. F. ROSS, *IEEE Trans. Instru. Meas.* **19** (1970) 377.
15. W. B. WEIR, *Proc. IEEE* **62** (1974) 33.
16. M. PERNET, X. OBRADORS, M. VALLET, T. HERNANDEZ and P. GERMI, *IEEE Trans. Magn.* **24** (1988) 1898.
17. R. GROSSINGER, *Phys. Status Solidi A* **66** (1981) 665; *J. Magn. Magn. Mater.* **28** (1982) 137.
18. M. SUGIMOTO, in "Ferromagnetic Materials," edited by E. P. Wohlfarth (North-Holland Publishing Company, 1982) Vol. 3, p. 305.
19. A. H. MORRISH, K. HANEDA and X. Z. ZHOU, in, "Nanophase Materials Synthesis-Properties-Application," edited by G. C. Hadjipanayis and R. W. Siegel (Kluwer Academic Publishers, Dordrecht/Boston/London, 1994) p. 515.
20. S. MØRUP, in edited by M. Takahashi, S. Maekawa, M. Gondo and H. Nosé (World Scientific Publishing Co. Ltd., Singapore, 1987).
21. S. MØRUP, M. B. MADSEN, J. FRANCK, J. VILLADSEN and C. J. W. KOCH, *J. Magn. Magn. Mater.* **40** (1983) 163.
22. Z. W. LI, C. K. ONG, Z. YANG, F. L. WEI, X. Z. ZHOU, J. H. ZHAO and A. H. MORRISH, *Phys. Rev.* B **62** (2000) 6530.
23. P. M. DeBAKKER, E. DeGRAVE, R. E. VANDENBERGHE and L. H. BOWEN, *Hyperfine Interac.* **54** (1990) 493.
24. K. HANEDA and A. H. MORRISH, *IEEE Trans. Magn.* **25** (1982) 2597.
25. K. HANEDA, X. Z. ZHOU and A. H. MORRISH, in edited by T. Yamaguchi and M. Abe "Ferrite: Proc. Int. Conf." (Japan Society of Powder Metallurgy, Japan, 1992), p. 1406.
26. H. IGARASHI and K. OKAZAKI, *J. Am. Cer. Soc.* **60** (1997) 51.
27. S. X. LI, *IEEE Trans. Magn.* **22** (1986) 14.
28. F. E. LUBORSKY, *J. Appl. Phys.* **32** (1961) 171.
29. A. GLOBUS and M. GUYOT, *Phys. Status Solidi* **52** (1972) 427.
30. J. VERWELL, Ferrites at radio frequencies, in: "magnetic Properties of Materials," edited by J. Smit (McGraw-Hill, 1971) p. 64.

Received 30 May 2003
and accepted 20 September 2004